The Fractal Geometry of the Universe

Joe Hollowed

April 30, 2020

1   Introduction

For at least the past century, it has been known that the galaxy space distribution is irregular, and tends toward a clustering-hierarchy. Even before the realization of the first surveys of the sky, it has long been accepted that the simplest conception of the universe as a timeless and uniform sea of stars and nebulae is incompatible with observations. Any modern student of cosmology is familiar with the coherent narrative that has now been constructed around these data, which describes the genesis and evolution of the large-scale galaxy distribution from inflation to a current era of accelerated expansion (ΛCDM).

A keystone of this story, one that is so familiar as to be often demoted by authors to triviality, is the *cosmological principle*. This postulate was formalized by Einstein and E.A. Milne (North, 1965), and (for our present purposes) states that the mass distribution on cosmological scales sources from a stationary random process, i.e. it is translationally invariant. It would certainly be scientifically responsible to seek empirical support for this assertion, if not develop a physical model which predicts it. The former was done definitively by the Sloan Digital Sky Survey (SDSS) (Tegmark et al., 2004; Hogg et al., 2005; Scrimgeour et al., 2012), though strong observational suggestions had been published before the turn of the century (Peebles, 1993).

At the same time, it is true that before useful observations reached the depth marked by the transition to large-scale homogeneity as found by SDSS, they first revealed a highly inhomogeneous clustering hierarchy of galaxies. This is clearly seen in Fig.1 (Peebles, 1993), which reproduces Carl Charlier's 1922 map of extragalactic objects (then "nebulae"), the most prominent feature being the Virgo cluster around the northern pole. After Charlier, Shapley then went on to conduct galaxy surveys over smaller yet deeper fields, which revealed new structures even *larger* than Virgo (Shapley, 1934), and Abell observed that galaxy clusters themselves tend to gather in concentrations, which he denoted as *superclusters* (Abell, 1958).
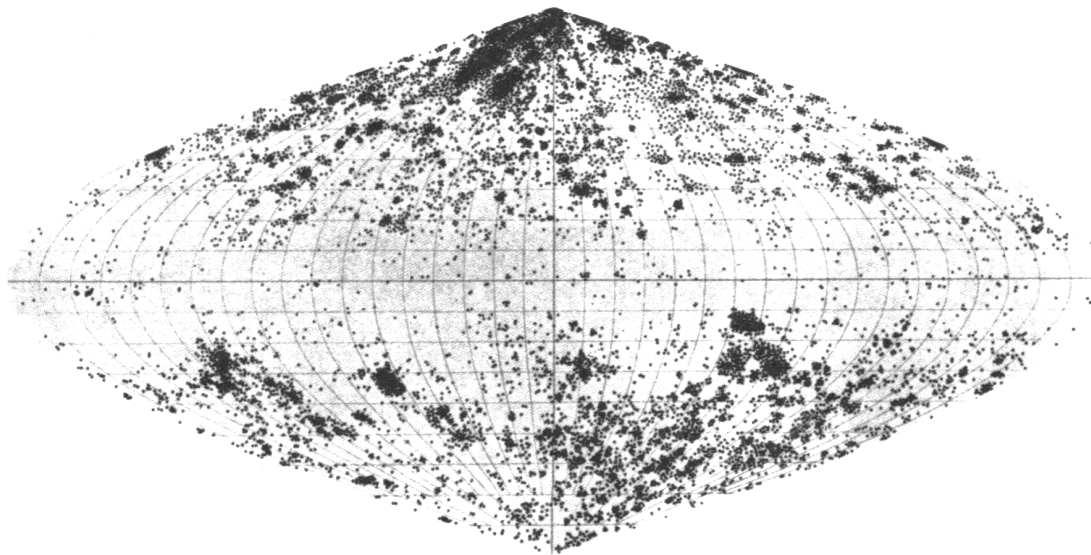

Figure 1: Charlier's 1922 map of "the nebulae"; the concentration of galaxies around the north pole is the Virgo cluster.

Despite the widespread acceptance of the cosmological principle during an experimentally-immature time in cosmology (1960's-1980's), there were still those who asked if the observations from Charlier to

Abell might suggest a pure scale-invariant cosmos, or that the clustering hierarchy might continue upward to arbitrarily large length scales. If so, then the galaxy distribution could be geometrically described as a *self-similar* or *scale-invariant fractal*. A small subset of the community steeped in these ideas for the latter part of the 20th century, and while there has never been proposed a theory which would generate and grow such a structure, various formal descriptions of the galaxy distribution in terms of their *fractal dimensions* have been developed (de Vaucouleurs, 1970; Pietronero, 1987; Mandelbrot, 1975).

Benoit B. Mandelbrot, in particular, was a foundational figure in the development of fractal geometry and its applications, and published his eminent text *The Fractal Geometry of Nature* (Mandelbrot (1977), from which the present work borrows figures, and even a title). There he lays out both his philosophical conceptions of the cosmological principle, and a numerical model for generating fractal universes which match observations in 2- and 3-point galaxy correlation functions. Ultimately, the elegant fractal picture of the cosmos is effectively ruled out, and Mandelbrot's model in particular is (fatally) tested against observations in Peebles (1993).

The remainder of this paper is organized as follows: Section 2 introduces important pieces of fractal geometry formalism. Section 3 describes how fractal models may be applied to the geometry of the cosmic web, and how they lead to a steady-state resolution to Olbers' paradox. It will conclude with a look at how Mandelbrot's Lévy flight fractal model for the galaxy distribution is ruled out via it's observationally-incompatible predictions for the angular correlation function. Section 3.4 will briefly discuss some modern descriptions and investigations into the self-similar regime of large-scale structure, i.e. the details of the clustering hierarchy.

Those readers interested enough to make it through even the introduction of this work know that models in violation of the cosmological principle are not often enthusiastically received in 2020. Still, the fractal model is mathematically interesting (I assert on aesthetic grounds), and the sequence of its conception and eventual remission is illuminating to the student scientist (perhaps even more so than the current era of ΛCDM systematics weed-wacking). Hence, this paper retains the historical flavor of this introduction throughout, and will necessarily be "out of date", by design.

2   Fractal Dimensions and Self-Similarity

A *fractal*, under a relaxed definition, is a "shape made of parts similar to the whole in some way" (Feder, 2013). This is exhibited in nature in a multitude of incarnations— a typical example is that of a Red Lady fern, whose pinnae resemble scaled down copies of the larger leaf from which they stem. We will see over the proceeding subsections that with the formal introductions of *Hausdorff* or *fractal dimensions*, a more precise and quantitative set of geometrical bounds for what constitutes a *fractal* will be obtained.

Briefly, fractals are objects for which a particular *measure* (e.g. lengths, volumes, densities) scales in a way that departs from the expectation derived from the object;s topology. In the case of the galaxy distribution, we will see in Section 3 that it is possible for a set of zero-dimensional objects (points) embedded in $\mathbb{R}^3$ to experience a density which scales with less than the spatial volume, even for sets which satisfy what we will call the *conditional cosmological principle*.

2.1   *The Richardson Effect*

An introduction to fractal geometry often begins with a case study of the *Richardson Effect*, so named for the observation that the measured coastline length of land masses on Earth *diverges* with a shrinking scale of measurement. To understand this, consider how we might attempt to empirically measure the length of a coastline. The most obvious method is to walk the length of the shore, carrying a ruler of length ϵ. The length is then

$$L(\epsilon) = N\epsilon \tag{1}$$

where N is the number of length-ϵ rulers required to span the distance. By choosing a particular length, we are in effect choosing a smoothing scale for the features of the coast— for very large ϵ, we need only

Figure 2: The northwest coastline of Washington state, traced from a 2018 sea level rise report by Miller et al. (2018). Notice that the coast looks nearly smooth on the western edge, while it becomes very detailed as the eye follows the Salish Sea inland. With increasing resolution (decreasing ϵ), we would find that the same can in fact be said of even the most apparently featureless portions of the coast.

move our ruler a handful of times to get a very crude estimate for L, while small ϵ will take us on a journey along every peninsula, and around every inlet. In general, $dL/d\epsilon < 0$. This is illustrated in Fig. 2, where a rendering of the northwest Washington coast is shown; the point is particularly salient on the right of the figure, where our choice of ϵ will strongly influence for how long we are meandering about the straits, sounds, and bays that surround Seattle.

We might expect that L converges upon some "true" coastline length in the limit $\epsilon \to 0$. However, this turns out not to be the case. There may exist some "stable" interval $\epsilon_- < \epsilon < \epsilon_+$ where L changes very little, as our scale is small enough to capture all macroscopic land features, but not yet small enough to care about individual stones. As soon as $\epsilon < \epsilon_-$, however, L increases again.

There are several other hypothetical methods of measurement of L described in Mandelbrot (1977) and Feder (2013), though the conclusion is always the same: the curve defined by the collection of points along a coastline is not *rectifiable*:

$$\lim_{\epsilon \to 0} L = \infty. \tag{2}$$

2.2 The Hausdorff dimension

For the utilitarian filling in tables for the encyclopedia, an arbitrarily (even anthropocentrically) chosen ϵ is no issue. As scientists, however, we'd much rather come up with some other way of objectively investigating the coast. Fortunately, this is exactly what mathematician Lewis Fry Richardson offers in his 1961 report giving empirical data on the rate of increase of L, as reproduced in Mandelbrot (1977) and shown in Fig. 3. Richardson's data shows that the relationship between L and ϵ in log-space is linear, as

$$L = \lambda \epsilon^{1-D} \tag{3}$$

where the number N of required rulers to span the coast at length ϵ is $\lambda \epsilon^{-D}$.

Fig. 3 delivers an important message; on the one hand, it affirms that a specific choice of ϵ is arbitrary, and on the other, it identifies the slope $1 - D$ as being a quantity that is unique per coast, and constant. That is, the quantity $1 - D$ is an *intrinsic* property of the 1-dimensional curve that constitutes a coastline as embedded in the 2-dimensional space of the Earth's surface. While Richardson did not himself have a theoretical interpretation for the parameters of Eq. 3 at the time, D is now understood to be the *fractal* or *Hausdorff dimension* of the curve.
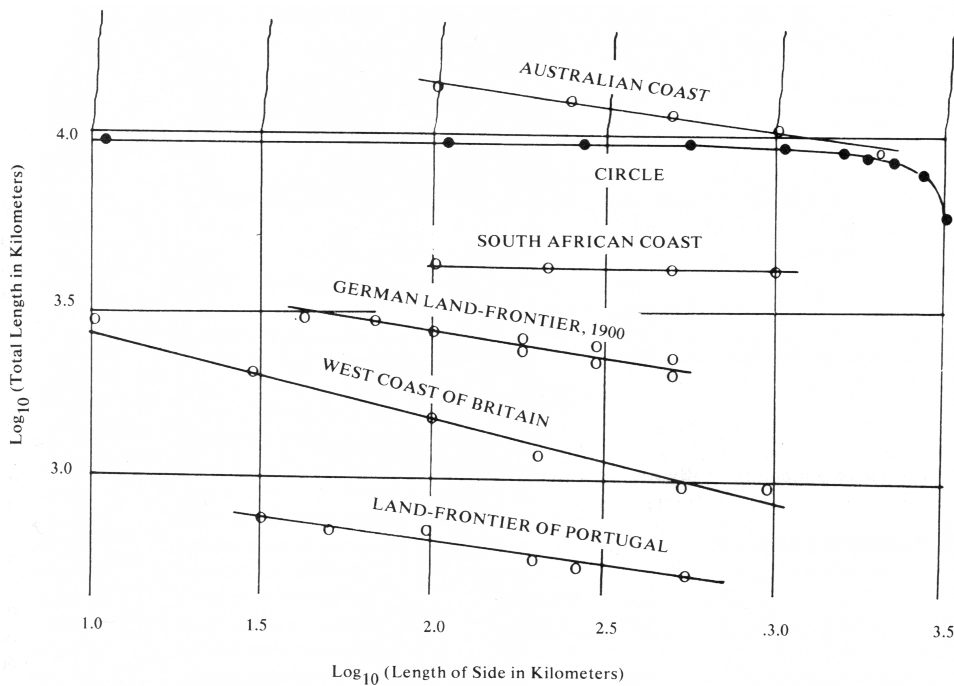
Figure 3: Richardson's data showing the lack of coastline length L convergence with measurement resolution. This figure is reproduced from Mandelbrot (1977), which adds a curve (black points) for the measure of a circle circumference, showing the rapid stabilization of L in the Euclidean case.

The statement is, then, that coastlines have a continual hierarchy of small-scale detail, which is resolved ad infinitum as $\epsilon \to 0$. Obviously, this is not true of all curves; for the well-tamed curves of standard Euclidean geometry, L will indeed stabilize to a true value. For example, the measure of the circumference of a circle of radius R converges rapidly as seen in the dark curve of Fig.3.

What exactly *is* the fractal dimension D, then? We can define a *measure M_d* of dimension d for a point set $\mathcal{S}$, as

$$M_d = \sum \gamma(d)\epsilon^d = \gamma(d)N(\epsilon)\epsilon^d \tag{4}$$

where $\gamma(d)$ is a geometrical factor (e.g. 1 for lines and planes, and multiples of π for discs, spheres, etc.), and N is as used above. In general, M_d will converge to either 0 or ∞ depending on the choice of d. We can understand this in the simple example of the measure (length) of a Euclidean curve. In that case, the topological dimension of the object is 1; if we try to measure its length ℓ with zero-dimensional points, we find it takes an infinite number, while if we try to measure ℓ with 2-dimensional planes, even one is too many. This immediately implies the existence of a *critical dimension D* where the asymptotic behavior of the measure transitions between the diverging and vanishing cases:

$$\lim_{\epsilon \to 0} M_d = \begin{cases} 0 & d > D \\ \infty & d < D \end{cases} \tag{5}$$

This formally defines the Hausdorff dimension, which we interpret as the fractal dimension of the coastlines as presented in Richardson's data. Familiar cases are $D = 1, 2, 3$ for lines, planes, and spheres/other finite volumes, respectively. We then see that, for Euclidean objects, the Hausdorff dimension D is always equivalent to the object's topological dimension D_T.

For fractals, D departs from the topological dimension of the object itself, as we already saw implied above (for coastline curves of $D_T = 1$, $1 - D > 0$). In the limit that that a coastline is *so* detailed that it fills the entire plane in which it is embedded, then the upper bound $D = 2$ is realized (a *Peano curve*). In other words, D must satisfy

$$D_T < D \leq E \tag{6}$$

4

for a fractal object of topological dimension D_T embedded in $\mathbb{R}^E$. With Eq. 6, we now have a more rigorous definition for a fractal as *any object whose Hausdorff dimension strictly exceeds its topological dimension.*

2.3 Self-Similarity

We now note some important symmetries, or invariances, of fractals. As discussed in 1, the motivating feature for modeling the galaxy distribution as a fractal is the clustering hierarchy of large-scale structure (LSS), where galaxies tend to concentrate into groups, groups into clusters, clusters into superclusters... and likewise in the negative for voids and sub-voids. In fact, it is this property that allows dark matter halos from modern cosmological simulations to be mapped onto tree-like data structures.

This suggests the use of a *scaling fractal* in modeling the geometry of LSS. To understand this, let us again consider the 1-dimensional Euclidean line. A line $\mathbf{x}$ through the point $\mathbf{x}_0$ in a direction $\hat{\mathbf{a}} = (a_1, a_2, a_3)$,

$$\mathbf{x} = \mathbf{x}_0 + t\hat{\mathbf{a}}, \quad -\infty < t < \infty \tag{7}$$

is invariant under translations along $\hat{\mathbf{a}}$, and thus invariant to length scale transformations $\mathbf{x} \to r\mathbf{x}$, (since this will only amount to translating $\mathbf{x}_0$, and t is continuous, in the definition above). Similarly, a 3-dimensional space is invariant under translations or rotations in any direction, and changes of scale. In general, as soon as we depart from a perfectly homogeneous point distribution, however, we must necessarily give up some of these symmetries— in constraining a 3-dimensional space to a sphere, for example, we retain rotational symmetry, but lose transnational and scaling invariance.

The galaxy distribution in the universe obviously fits into this category; it does not, up to scale of ~ 100Mpc, have translational or rotational invariance. It does, however, have notable scale-invariance. It turns out that there are a wealth of fractals that satisfy this condition, and are thus candidates for describing large-scale clustering, though we defer a detailed discussion to Section 3. For now, suffice it to say that a fractal is similar-to-itself on varying length scales, or *self-similar* under the condition that the Hausdorff dimension of the object equal the *similarity dimension D_S*.
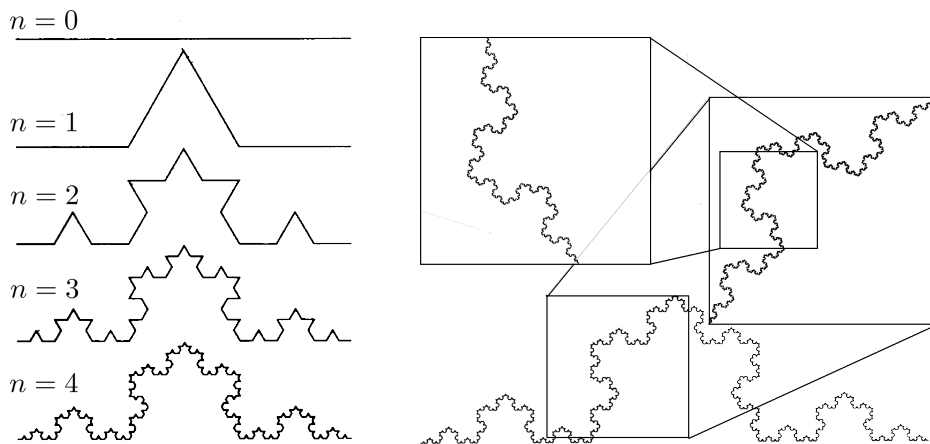

Figure 4: The 1.262-dimensional self-similar Koch curve fractal. Here we visually demonstrate that the appearance of the object is invariant to length scaling, and has infinite detail at any chosen location. This property is shared with coastlines (at least to the length scale of atoms), and gives rise to the divergence of L with measurement resolution ϵ.

We leave a technical definition of D_S to Feder (2013)— where the interested reader is encouraged to look— as it would necessitate the cumbersome definition of a few more quantities. Fortunately, these ideas can be understood intuitively, especially when considering the simple example of the *Koch curve*, whose construction and detail is shown in Fig.4. This scale-invariant curve ($D_T = 1$) is constructed, starting at the *initiator* (labelled as $n = 0$), by making successive insertions of the *generator* (labelled as $n = 1$) shape to all straight-line segments. It has

$$D = D_S = \ln 3 / \ln 4 \simeq 1.262, \tag{8}$$

the measured length of which would scale with resolution (and arbitrary normalization) as

$$L(\epsilon) = \lambda \epsilon^{0.262}. \tag{9}$$

One could imagine a similar figure being produced for a higher dimensional fractal, or even for observed or simulated realizations of the cosmos itself (which is what is done in Fig. 7). For the remainder of this paper, we will only be discussing self-similar fractals, and assume that all further instances of D imply $D = D_S$.

3 Fractal Expressions of the Large Scale Galaxy Distribution

Given the language of Section 2, the large-scale galaxy distribution we take as being composed of zero-dimensional point particles, so $D_T = 0$, embedded in $\mathbb{R}^E$ where obviously $E = 3$. If the matter distribution is to be modeled as a fractal, then it has a fractal dimension with

$$0 < D \le 3 \tag{10}$$

where the rightmost inequality is saturated, $D = 3$, if the galaxy distribution becomes a homogeneous fluid (i.e. has transnational and rotational symmetry, or satisfies the cosmological principle). But, if indeed the distribution is a fractal, then we should identify some analog to the coastline length L that will exhibit interesting scaling properties with resolution. That quantity, as we will see, is the average mass density ρ. For any galaxy distribution that maintains a fractal dimension $D < 3$ up to arbitrarily large length scales, then the the average density of the universe will vanish, rather than converge upon a "global" value, which the Freidmann equation supposes.

As a reminder, and as emphasized in 1, $D = 3$ was not measured observationally during the times that the models to be discussed over the following subsections were developed. Additionally, a universe with zero global density potentially has several nice properties from the perspective of a 20th-century steady-state cosmologist; it prevents gravitaional collapse of such a universe, and also solves Olbers' Paradox, as discussed next.

3.1 *Resolving Olbers' paradox*

Olbers' Paradox states that the observation of a dark night sky demands a cosmological explanation (so called a "paradox" since it was considered since at least the times of Kepler, when the simplest assumption of the universe as eternal and infinite dominated). The reader should recall that the quantitative statement of the paradox is as follows: The total flux F_T received by an observer positioned within a uniform sea of stars (or galaxies) of luminosity L_* (flux F_*) at a density n_* out to a distance R takes the form

$$F_T = \int n_* F_* r^2 dr d\Omega = \int_0^R 4\pi n_* F_* r^2 dr \tag{11}$$

$$= \int_0^R n_* L_* dr = n_* L_* R \tag{12}$$

which diverges for $R \to \infty$. The modern solutions to this problem come in part from cosmological redshift (expansion of the universe), but mostly from the finite age of the universe, which sets an upper bound on our particle horizon. Less often mentioned is that *geometrical* solutions are also potentially successful, even ones that maintain a restricted *conditional cosmological principle* (see Section 3.2).

To see how this works, consider the mean number of galaxies within a sphere of radius r from the observer, $N(< r)$, normalized by A. For a self-similar fractal of dimension D, this statistic, and thus the number density $n(< r)$, scale as a power law:

$$N(< r) = Ar^d \tag{13}$$

$$\implies n(< r) = \frac{N(< r)}{V(r)} = Ar^{-\gamma}, \quad \gamma = 3 - D \tag{14}$$

The reader should note the similarity here with Eq.3 of the Richardson Effect, though the behavior is now in the opposite direction, where we consider $r \to \infty$. The expression for F_T is then

$$F_T = \int_0^R n(<r)L_* r^2 dr = \int_0^R AL_* r^{-\gamma} dr = \frac{AL_* R^{1-\gamma}}{1-\gamma}.$$ (15)

We then see that Olbers' Paradox is solved, i.e. F_T converges for $R \to \infty$ for

$$\gamma < 1 \implies D < 2,$$ (16)

even for an infinitely old and static universe.

3.2 *Random fractals and Mandelbrot's Lévy flight*

Though the previous section demonstrates the convergence of the flux from the sky for a galaxy distribution of fractal dimension $D < 2$ for a static and eternal universe, proof of the contrary to the latter (i.e. Big Bang theory) need not rule out the fractal picture. That is, as long as we have a specific model of fractal clustering which is compatible with the expanding universe, even if a theory for its genesis is unknown, we can still ask if it is realized in the cosmos on purely geometric grounds. A model fitting this description was introduced in cosmology by Mandelbrot (1975), and is described at length in Mandelbrot (1977) and Peebles (1993). To discuss it, we should first have in hand the idea of *random* fractals.

Referring back to Fig.4, note that each successive generation in the construction of the Koch curve (labelled by n) has it's smallest features decrease in size by a discrete scale factor. There are many contrived fractals occupying $\mathbb{R}^3$ that display the same property (perhaps the best known example is *Cantor dust*). This phenomenon is referred to as *stratification*, and clustering fractals that exhibit discrete levels of scale in their hierarchy are said to be *stratified*.

The galaxy distribution can be thought of in spectral terms when Fourier transforming the two-point correlation function ξ into the *power spectrum $P(k)$*. As the reader is likely familiar, the power spectrum does not have spikes of power at particular scales... in other words, the density contrast field in k-space $\delta(\mathbf{k})$ is a continuous function, and says that present-day structure has grown from density perturbations at *all* scales.

Given this, the mass distribution certainly cannot be represented by a stratified fractal. Instead, we require a fractal for which the construction process is inherently *random*, and thus the associated fractal dimension and scaling properties are statistically defined and measured. Perhaps the most familiar example to the physicist is Brownian motion, or random walks. As a brief refresher, a typical random walk in one dimension works by choosing a distance δ to step in time intervals τ, where δ is chosen from a Gaussian:

$$p(\delta, \tau) = \frac{1}{\sqrt{4\pi D\tau}} \exp\left(-\frac{\delta}{4D\tau}\right).$$ (17)

D is the *diffusion coefficient*, given by the *Einstein relation* in terms of the process variance $\langle \delta^2 \rangle$ as

$$D = \frac{1}{2\tau}\langle \delta^2 \rangle$$ (18)

Note that the step distances and variance depend on the temporal resolution τ. If we increase the temporal resolution of our Brownian walk, we recover another set of step lengths δ that remain Gaussian distributed, though the variance has increased. It is in this sense that the Brownian process is scale-invariant, and explicitly un-stratified, as δ varies smoothly. Hence, we can use it as a vehicle by which to create a fractal "dust" (set of $D_T = 0$ points) which may successfully model the galaxy distribution.

Now brings us back to the method described in Mandelbrot (1975). Here, Mandelbrot showcases a $D_T = 0$ fractal built from a *Lévy flight* random process. This is similar to the random walk, although the

distribution from which the steps of the random walk are drawn is no longer Gaussian. Rather, a Pareto distribution is used, whose survival function is

$$p(> \delta) = \begin{cases} (\delta_0/\delta)^D & \delta \geq \delta_0 \\ 1 & \delta < \delta_0 \end{cases} \tag{19}$$

The normalization δ_0 and scale parameter D (fractal dimension) of this distribution are adjusted to fit the two-point correlation function ξ on small scales. The performance of the model after doing so is discussed in Section 3.3. Example output of the Lévy flight operating to create a clustering fractal dust from Mandelbrot (1977) is shown in Fig. 5.

In addition, I have written my own Lévy flight, which is shown in 6. Here, I've run two flights while varying the fractal dimension D from $D = 1.26$ to $D = 1.5$. The steps of the flight are taken isotropically in $\mathbb{R}^3$, with their magnitudes drawn from the Pareto PDF associated with Eq. 19. The same random seed is used on each run, and thus the overall shape of the resulting distribution is similar, with the higher dimensional set having more notable detail (just as expected). Both a projection of the 3-dimensional tracks are shown, as well as the stops of the flight in angular space. The angular projection was done with respect to an "observer", shown as a red dot, placed in a low-density cluster, as identified by a Gaussian kernel density estimator. The right side of the figure displays the statistical scale invariance of the output.

In both figures 5 and 6 The result is statistically scale-invariant, since a shrinking of the time stepping with a fixed random seed would serve to produce more detailed clustering, while allowing the algorithm to run longer would begin to construct larger clusters entirely. In this way, a cluster hierarchy is arrived at, despite the fact that there is no explicit scale-invariant condition imposed, other than the built-in self-similarity of the Lévy process.
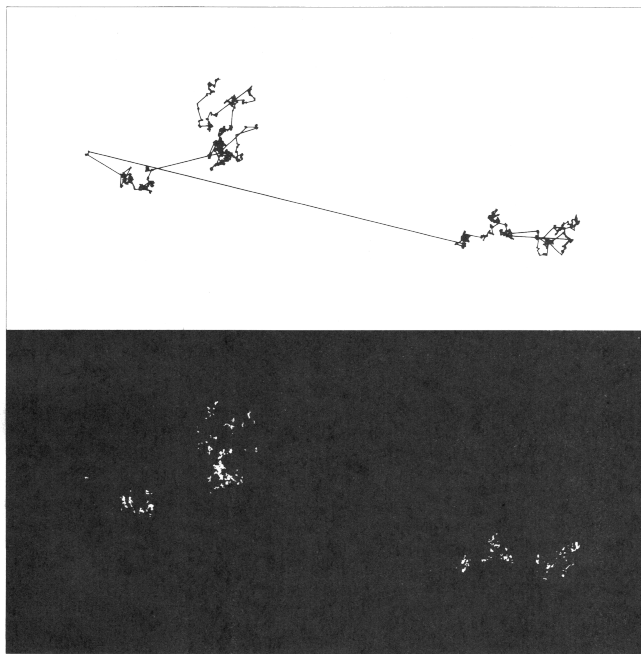

Figure 5: Example output of the Lévy flight clustering hierarchical model descried in the text, reproduced from Mandelbrot (1977). The walker was allowed to explore 3-dimensional space, and it's plane projection is shown here. The fractal dimension is $D = 1.26$. The top panel shows the record of the process, while the bottom panel shows just the resulting point set, which would represent the galaxy distribution.

If we were to let a process run in this way until it spanned a spherical volume that we might consider as the "observable universe", then clearly it will *not* satisfy the cosmological principle, in that the clustering hierarchy continues forever, and no scale of homogeneity exists. It does, however, satisfy what Mandelbrot calls the *conditional cosmological principle*.
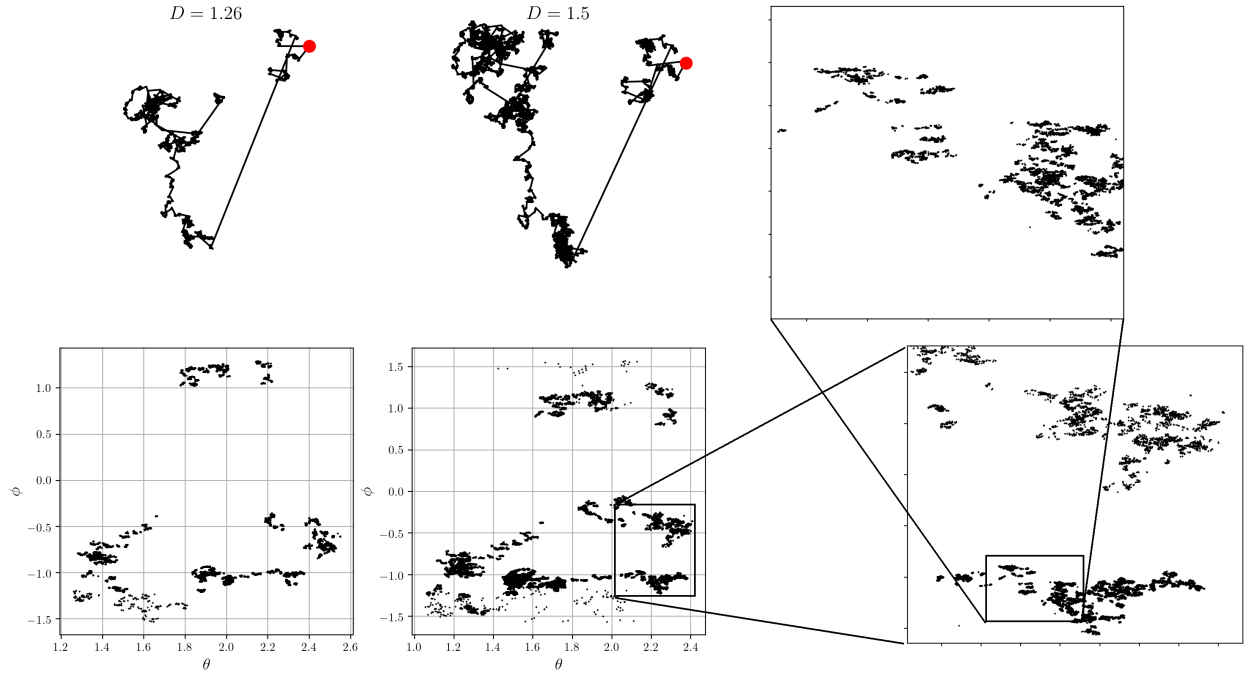
Figure 6: My own realization of a point distribution as resulting from a random Lévy flight. Two fractal dimensions are shown of the same density field at $D = 1.26$ (left) and $D = 1.5$(right). The lower dimensional instance corresponds to Mandelbrot's model, and the true fractal dimension of the observed galaxy distribution at small scales. The higher dimensional instance includes extra panels (right) which progressively zoom in on a particular structure, highlighting the self-similarity of the hierarchical clustering pattern that is emergent from this process. The stops of the flight are shown projected into angular space in the lower panels, which are taken with respect to an "observer" placed at a low-density location within the flight (i.e. at a *conditioned* location, in Mandelbrot's language of the conditional cosmological principle).

The conditional cosmological principle states that the probability distribution of mass is independent for all frames of reference which satisfy the condition that they are "material" (Mandelbrot, 1977). That is, all possible observers will measure the same statistical properties of the universe, where "observers" are assumed not to exist within the voids of the clustering hierarchy. That is, the fractal is not generally translationally invariant, though measures of it's mass within a radius R taken from *within* the fractal itself are statistically stationary.

Importantly, this principle remains constant when considering either the case that the global density of the universe converges, or vanishes. Mandelbrot regards this as philosophically attractive, in that it concerns everything that is observable, and leaves the stronger claim of general transnational invariance to be identified as the "working hypothesis" of a *strong cosmological principle*.

3.3   *Statistical tests of large-scale homogeneity*

We will now demonstrate that while the model of Section 3.2 can be tuned to match important summary statistics of the galaxy distribution in the universe on local scales, it can be proven observationally that the self-similarity cannot continue to arbitrarily large scales. We already know that this must be true in the verification of the cosmological principle as achieved by SDSS and discussed in Section 1, though an earlier argument falsifying the fractal model is presented in Peebles (1993).

First, we note that the fractal dimension of the galaxy distribution on small-scales was measured from observational data decades ago by de Vaucouleurs (1970), the best estimate via indirect evidence being $D = 1.23$. This is again reported to higher confidence by Peebles (1993); the reduced two-point correlation function for galaxies is now established to well-approximate a power low on small-scales

$$\xi(r) = (r_o/r)^\gamma \tag{20}$$

where the best-fit parameters before SDSS were

$$\gamma = 1.77 \pm 0.04, \quad r_0 = 5.4 \pm 1 h^{-1} \text{Mpc}. \tag{21}$$

ξ is proportional to the local density for $r < r_0$, so recalling Eq.14, the fractal dimension is $D = 1.23 \pm 0.04$.

On these small scales, this simple power-law model is quite similar to Mandelbrot's Lévy flight, when it is tuned. Indeed, Mandelbrot (1977) even reports that the Lévy model fits well to the three-point correlation function ζ. That is, the geometry of the galaxy distribution on cosmologically local scales *is* a self-similar clustering hierarchy that may be described in fractal formalism. The next question to ask, then , is if it retains it's impressive performance to larger scales.

There are several observable vehicles by which to investigate this question; a study of the cosmic X-ray background anisotropy yields a large-scale value for the fractal dimension $D \approx 2.999$. In other words, in agreement with Sloan, no, the galaxy distribution is not a scale-invariant fractal beyond the scale of the largest observed clusters, and converges upon a homogeneous fluid with a finite global density.

Let's now see, in some (though not full) detail, another approach which considers the *angular* two-point function $w(\theta)$. To begin, we consider a magnitude-limited galaxy sample. In that case, the mean number of galaxies per steredian brighter than a specific flux density f for a *homogenous* distribution is

$$\mathcal{N}(> f) = \int_0^\infty n r^2 \psi(4\pi r^2 f L_*) dr \tag{22}$$

$$= n \frac{(3/2 + \alpha)!}{3} \left(\frac{L_*}{4\pi f} \right)^{3/2} \tag{23}$$

where ψ is the luminosity function, and the result on the second line comes when setting ψ to the commonly used Schechter form. For the fractal model with the space density defined as in Eq. 14, $\mathcal{N}$ is

$$\mathcal{N}(> f) = 2C \int_0^\infty r^{2-\gamma} \psi(4\pi r^2 f / L_*) dr \tag{24}$$

$$= 2C \frac{(3/2 - \gamma/2 + \alpha)!}{3 - \gamma} \left(\frac{L_*}{4\pi f} \right)^{(3-\gamma)/2} \tag{25}$$

with C as a normalization constant to be set by observations. In sparing the details (see Peebles (1993)) and exporting the important result, it can be shown that when computing the angular two-point correlation functions $w(\theta)$ arising from these number densities, the extra factor of $(L_*/4\pi f)^{-\gamma/2}$ removes all dependence of f, the flux density, or equivalently limiting magnitude m of the sample, from the fractal angular two-point function. That is, with the homogeneous and fractal angular correlation functions $w_h(\theta)$ and $w_f(\theta)$, respectively, we find

$$w_h(\theta) \propto \left(\frac{4\pi r_0^2 f}{L_*} \right)^{\gamma/2}, \quad w_f(\theta) \propto \left(\frac{4\pi r_0^2 f}{L_*} \right)^{\gamma/2 - \gamma/2} = 1. \tag{26}$$

The former is the behavior that is observed in the real galaxy distribution, i.e. the magnitude of the angular two-point function falls notably with redshift. This is expected of a homogeneous distribution, as fixed angular sizes for more and more distant samples of LSS should see it's angular fluctuations average out. On the other hand, the scale-invariant construction of the cosmic web is just that, and will only reveal larger and larger clusters and voids as observations are made deeper.

The fact that this is not seen in the data is a fatal blow to Mandelbrot's fractal model, unless the true fratal dimension d is *exceedingly* close to to limiting case of $D = E = 3$. In other words, we can be confident that the galaxy space distribution is indeed a stationary random process, which satisfies both the conditional, and more general cosmological principles, as discussed in 3.2.

3.4 Modern explorations of the scale-invariant regime

Finally, we very briefly discuss modern computationally-assisted investigations of the scale-invariant regime, mainly for entertaining purposes. While observations have shown the purely scale-invariant picture of the cosmic web to be incompatible with observations on the largest scales, it is still a useful geometrical framework within which to discuss intermediate scales in the cosmos, before the scale of homogeneity identified at ~ 70 Mpc by SDSS.

A detailed capacity for these kind of studies has been enabled by high-performance gravitational N-body codes, which simulate the growth of large-scale structure at impressive dynamic ranges. Shown in Fig. 7 is a figure from a computational study on cosmic void composition and dynamics (Aragon-Calvo and Szalay, 2012). Here, a cosmological N-body simulation is run, wherein underdensities in the matter field called *voids* were identified. Then, a chosen void is isolated, and it's constituent particle positions and velocities are used as initial conditions to run a new higher-resolution (and thus higher mass contrast) simulation. In this way, a structure very similar to the larger cosmic web is revealed within the void, thus demonstrating the self-similarity of the cosmos on these scales.
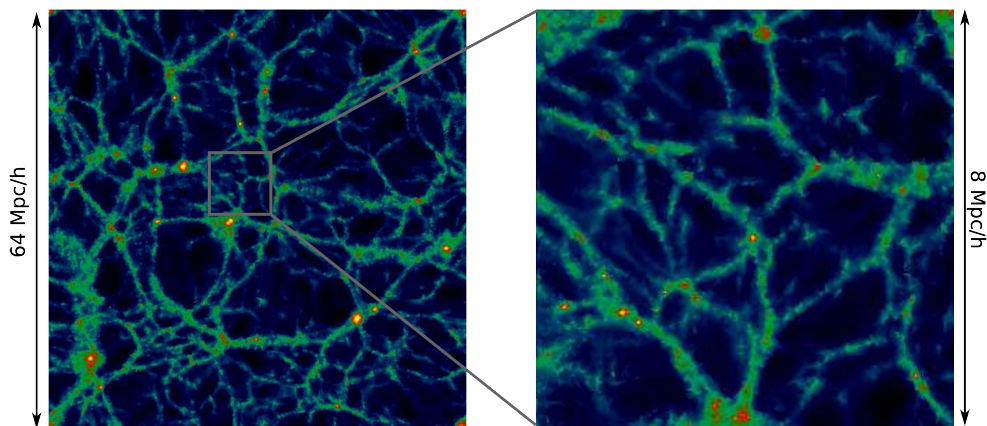

Figure 7: Figure reproduced from Aragon-Calvo and Szalay (2012), showing a 64 Mpch^{-1} slice of the cosmic web in a ΛCDM cosmology (left), and a higher-contrast zoom-in on an identified void (right).

Many more such simulation campaigns are currently underway, and now have the high dynamic range in order to resolve galaxy-scale objects, where the scale-invariance concludes on local scales, while simultaneously being large enough to sample the scale of homogeneity 10-100 times (e.g. Nelson et al. (2019) and Heitmann et al. (2019)). The creation of these high fidelity data products is allowing analysis on the topology/morphology of the cosmic web itself, e.g. Libeskind et al. (2018) and Ramachandra and Shandarin (2017).

4 Conclusion and Acknowledgments

In this report, we have reviewed fractal models of the large-scale galaxy distribution. We have discussed the historical motivation for such models, in particular how an apparently scale-invariant clustering hierarchy was revealed by deepening observations during the early 20th century.

During this time, specific geometric descriptions of fractal realizations of the cosmic web were developed, most notably by Mandelbrot. In order to introduce and describe such models, this report reviews the fundamentals of fractal geometry. It was shown that observable tests can be developed for testing the plausibility of these models, at least one of which passes with flying colors (Olbers' Paradox), while others fail catastrophically (i.e. the redshift-dependence of the angular two-point correlation function). Nevertheless, the self-similarity of the cosmic web does exist between certain cutoff scales, and it is enlightening to be able to consider the large-scale structure of the universe in these terms.

This paper was written as a final project for Physics 525: Early Universe Cosmology at the University of Michigan. I'm grateful for the guidance and support of Professor Fred Adams, my classmates for input and attention of this work's presentation, as well as three authors in particular (Mandelbrot, 1977; Feder, 2013; Peebles, 1993), without whom it would have been much more difficult to navigate this slightly archaic topic.

References

Abell, George O. (May 1958). "The Distribution of Rich Clusters of Galaxies." In: 3, p. 211. DOI: 10.1086/190036.

Aragon-Calvo, Miguel and Alexander Szalay (Mar. 2012). "The Hierarchical Structure and Dynamics of Voids". In: *Monthly Notices of the Royal Astronomical Society* 428. DOI: 10.1093/mnras/sts281.

de Vaucouleurs, G. (Feb. 1970). "The Case for a Hierarchical Cosmology". In: *Science* 167.3922, pp. 1203–1213. DOI: 10.1126/science.167.3922.1203.

Feder, J. (2013). *Fractals*. Physics of Solids and Liquids. Springer US. ISBN: 9781489921246. URL: https://books.google.com/books?id=mgvyBwAAQBAJ.

Heitmann, Katrin et al. (Nov. 2019). "The Outer Rim Simulation: A Path to Many-core Supercomputers". In: 245.1, 16, p. 16. DOI: 10.3847/1538-4365/ab4da1. arXiv: 1904.11970 [astro-ph.CO].

Hogg, David W. et al. (May 2005). "Cosmic Homogeneity Demonstrated with Luminous Red Galaxies". In: 624.1, pp. 54–58. DOI: 10.1086/429084. arXiv: astro-ph/0411197 [astro-ph].

Libeskind, Noam I. et al. (Jan. 2018). "Tracing the cosmic web". In: 473.1, pp. 1195–1217. DOI: 10.1093/mnras/stx1976. arXiv: 1705.03021 [astro-ph.CO].

Mandelbrot, B. (June 1975). "Sur un modèle décomposable d'univers hiérarchisé: déduction des corrélations galactiques sur la sphère céleste." In: *Academie des Sciences Paris Comptes Rendus Serie Sciences Mathematiques* 280.22, pp. 1551–1554.

Mandelbrot, B. (1977). *The Fractal Geometry of Nature*.

Miller, Ian et al. (Dec. 2018). "Projected Sea Level Rise for Washington State – A 2018 Assessment." In: DOI: 10.13140/RG.2.2.30282.21440.

Nelson, Dylan et al. (May 2019). "The IllustrisTNG simulations: public data release". In: *Computational Astrophysics and Cosmology* 6.1, 2, p. 2. DOI: 10.1186/s40668-019-0028-x. arXiv: 1812.05609 [astro-ph.GA].

North, J. D. (1965). *The measure of the universe. A history of modern cosmology*.

Peebles, P. J. E. (1993). *Principles of Physical Cosmology*.

Pietronero, L. (Aug. 1987). "The fractal structure of the universe: Correlations of galaxies and clusters and the average mass density". In: *Physica A Statistical Mechanics and its Applications* 144.2-3, pp. 257–284. DOI: 10.1016/0378-4371(87)90191-9.

Ramachandra, Nesar S. and Sergei F. Shandarin (May 2017). "Topology and geometry of the dark matter web: A multi-stream view". In: 467.2, pp. 1748–1762. DOI: 10.1093/mnras/stx183. arXiv: 1608.05469 [astro-ph.CO].

Scrimgeour, Morag I. et al. (Sept. 2012). "The WiggleZ Dark Energy Survey: the transition to large-scale cosmic homogeneity". In: 425.1, pp. 116–134. DOI: 10.1111/j.1365-2966.2012.21402.x. arXiv: 1205.6812 [astro-ph.CO].

Shapley, Harlow (June 1934). "On some structural features of the metagalaxy (George Darwin Lecture)". In: 94, pp. 791–816. DOI: 10.1093/mnras/94.9.791.

Tegmark, Max et al. (May 2004). "The Three-Dimensional Power Spectrum of Galaxies from the Sloan Digital Sky Survey". In: 606.2, pp. 702–740. DOI: 10.1086/382125. arXiv: astro-ph/0310725 [astro-ph].